


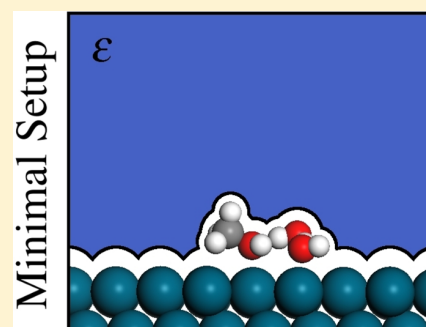
Solvation Effects on Methanol Decomposition on Pd(111), Pt(111), and Ru(0001)

Miquel Garcia-Ratés,*[✉] Rodrigo García-Muelas,[✉] and Núria López*[✉]

Institute of Chemical Research of Catalonia (ICIQ), The Barcelona Institute of Science and Technology, Avinguda dels Països Catalans 16, 43007 Tarragona, Spain

 Supporting Information

ABSTRACT: Solvation is crucial in many chemical and electrochemical processes related to alcohol conversion on metal surfaces. Particularly, understanding the dehydrogenation mechanism of methanol on solvated Pd, Pt, and Ru surfaces could allow the design of efficient methanol fuel cells. The large computational cost related to adopting an explicit solvation approach into density functional theory can be reduced drastically by using implicit solvation methods. In this study, we use our recently developed continuum solvation model (MGCM) to elucidate the minimum number of explicit water molecules to add to the solvated methanol/metal surface systems to reproduce experimental data with an optimized balance between time and reliability. Our results stress the importance of adding two explicit water molecules, especially for the case of Ru surfaces. For this later system, we provide a first insight into the decomposition mechanism of methanol using first-principles calculations. Our predictions can be then a useful reference for future studies that aim at designing more efficient heterogeneous catalysts with solvents.



■ INTRODUCTION

Biomass-derived compounds have received increasing attention in recent years as an alternative source of energy to fossil fuels.¹ Commonly biomass resources contain significant amounts of water. To avoid the complexity of long carbon polyalcohols, studies have been centered in surrogates, small alcohols, that already are of technological interest. Among such compounds, methanol, the simplest alcohol, has many advantages as energy carrier due to its high hydrogen content, availability, low cost, and ease of transport and storage. The use of methanol as a fuel is based on the so-called fuel-cell technology with potential applications in portable power and electric vehicles.² Direct methanol fuel cells (DMFCs) are used to decompose methanol to produce electricity. On the anode side of the DMFC methanol is oxidized on a metal catalyst such as platinum (Pt), palladium (Pd), or ruthenium (Ru) in an aqueous environment.² Water plays then a key role on the surface chemistry in DMFCs as it interacts with the adsorbate through hydrogen bonds, short-, and long-range interactions, and it modifies the number of available active sites on the metal catalyst. Therefore, should an active and selective catalyst be designed, the effect of the environment is to be considered carefully.

Density functional theory (DFT) has been employed extensively in methanol decomposition on metal surfaces.³ Studies of methanol adsorption on metal/vacuum and metal/water interfaces suggest that the methanol dehydrogenation pathway depends strongly on the environment. While experiments in ultrahigh vacuum (UHV) show that the adsorption of methanol on Pt and Ru surfaces starts with the O–H scission,^{4,5} theoretical studies under the same conditions lead

to different reaction pathways. For instance, Desai et al.⁶ studied the adsorption of methanol over Pt(111) surfaces in vacuum and observed that dehydrogenation pathways starting via the activation of the C–H bond are favored. A similar pathway for methanol decomposition on Pt(111) was suggested by Greeley and Mavrikakis through microkinetic modeling based on first-principles results.⁷ DFT-based results for the case of methanol adsorbed on Pd, Pt, and Ru surfaces in vacuum show that several C–H bond breakings occur before O–H scission. However, the formation of adsorbed methanol clusters is favored, and this promotes the O–H bond breaking.⁸ A good agreement is found between the results obtained from experiments and theoretical studies when aqueous methanol decomposition is considered. In this case, the initial step in the reaction pathway is the C–H bond cleavage.^{9–11} Neurock et al.¹² studied the dehydrogenation pathway from CH₃OH to CO on Pt(111) in the presence of explicit water molecules through DFT calculations. All dehydrogenation steps were more exothermic than in vacuum. In this case, CH_xOH intermediates are stabilized by hydrogen bonding with nearby H₂O and H₃O⁺ species, and then the C–H bond cleavage is favored over the O–H bond breaking during the reaction path. Similar results were reported by Hartnig and Spohr¹³ who observed that O–H bond dissociation does not occur when methanol is hydrogen-bonded to a water molecule. However,

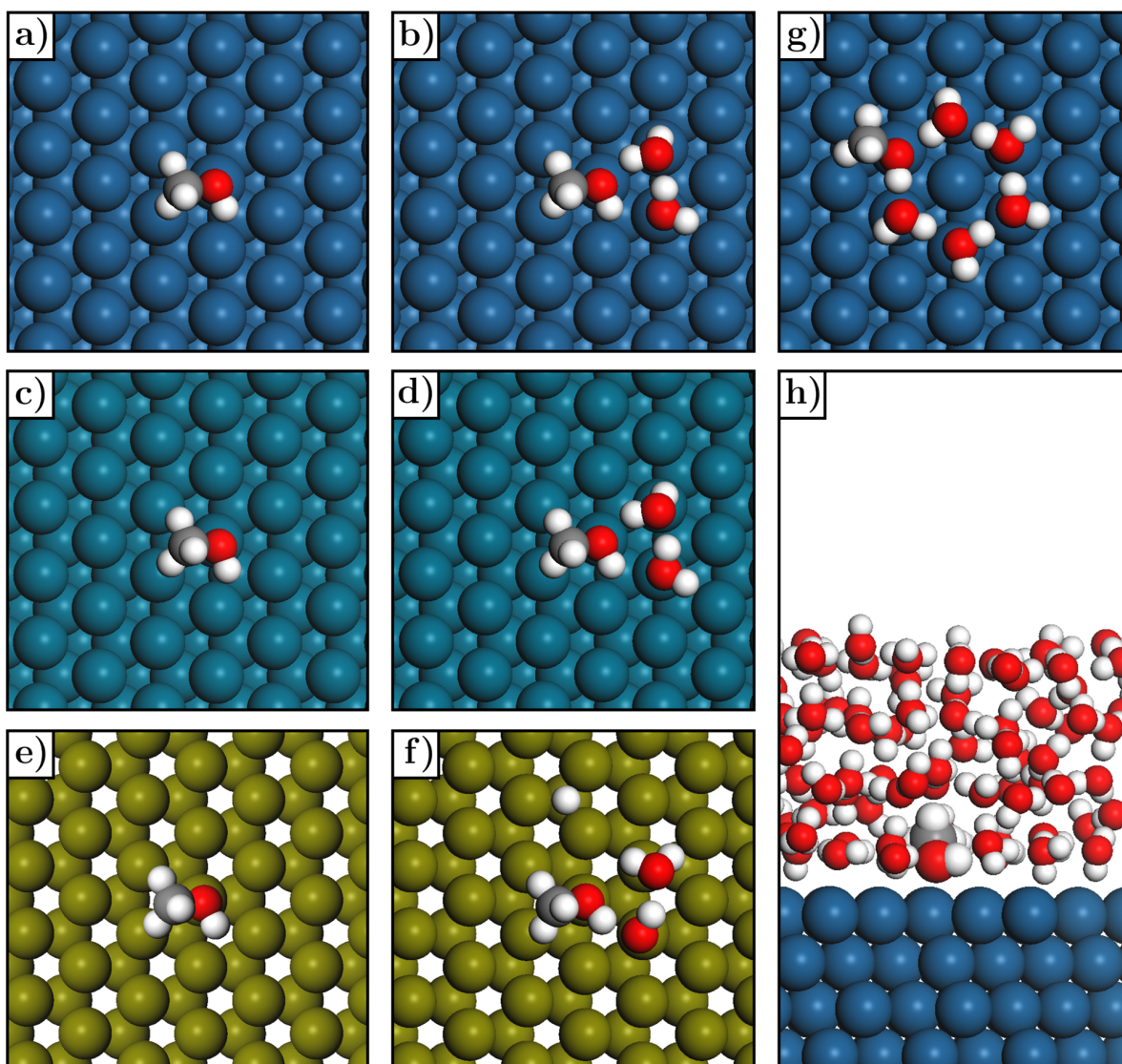


Figure 1. Models employed to study the adsorption of methanol on Pt, Pd, and Ru surfaces. Left panels (a, c, e) correspond to the CS (Pt(111) top, Pd(111) middle, and Ru(0001) bottom), while central panels (b, d, f) correspond to the S2W. Right panels correspond to the SSWR (g) and S71W (h) systems. For this last system, the radii of methanol atoms have been increased to distinguish the adsorbate from water molecules. Blue, turquoise, and golden spheres stand for platinum, palladium and ruthenium atoms, respectively, while red accounts for oxygen, white for hydrogen, and gray for carbon.

these studies mainly consider explicit molecules, and long-range solvent effects were not introduced.

Considering solvation effects in first-principles calculations is, nevertheless, a delicate issue. Explicit solvent modeling involves long-time scale molecular dynamics (MD) simulations as physical quantities should be averaged to compute the thermodynamic properties of interest.¹⁴ This results in an unaffordable computational cost for most of the systems of interest. However, the hydrogen bond stabilization of the adsorbed methanol comes mainly from the water molecules surrounding it and from those solvating the metal surface. In fact, water molecules located in the bulk, far away from the adsorption site, will have a residual effect on the methanol decomposition pathway. Thus, an alternative approach is to treat the solvent as a structureless continuum medium characterized by the value of its dielectric permittivity, while the solute and the nearby water molecules are treated through

quantum mechanics. This strategy, known as implicit solvation,¹⁵ reduces drastically the computational cost of the calculations without affecting the accuracy of the computed physical quantities. In this context, we have recently developed a continuum solvation model into the Vienna ab Initio Simulation Package (VASP),¹⁶ a plane-wave based electronic structure code, VASP-MGCM (VASP-Multigrid Continuum Model).¹⁷ The model solves the electrostatic problem through a multigrid solver and has been tested for a large number of isolated and adsorbed molecules on metal surfaces with a good agreement between experimental and simulation data. The key point in this type of calculations is to determine the number of solvent molecules to add to the simulation box.^{18,19} On the one hand, if no explicit solvent molecules are considered, the solute adsorption geometry can differ from the true configuration as the short-range polarization of the adsorbate is not properly described.²⁰ This leads to wrong estimates for thermodynamic

and kinetic parameters. On the other hand, adding a large number of solvent molecules results in a high computational cost and does not necessarily improve substantially the accuracy of the results with respect to the case where we consider a few number of explicit molecules.²¹ Several studies have adopted a combined explicit/implicit solvation approach to study different reactions on Pt(111) and its alloys. This is the case of the oxygen reduction reaction (ORR),^{20,22,23} the adsorption of H, O, and OH,²⁴ and the H₂O interactions with CO and sugar alcohols.²⁵ Although these studies provide relevant information about the reaction mechanisms of organic molecules on Pt(111) under solvation, the suitability of the explicit/implicit solvent approach has not been extensively studied for other metal surfaces like Pd(111) or Ru(0001).

In the present work, we have studied the effect of the solvent on the decomposition of methanol to formaldehyde on Pd(111), Pt(111), and Ru(0001) through DFT calculations. Our aim is not only to report the mechanisms of methanol dehydrogenation on metal surfaces under solvation, thus closer to the DMFC working conditions, but more importantly, to identify a minimum system setup to describe solvation effects accurately at the lowest computational cost. First of all, we demonstrate that the addition of two water molecules on the Pd and Pt surfaces permits to reproduce experimental and simulation results where the methanol C–H bond breaking is the preferred first dehydrogenation step under solvation. In addition, we report for the first time the mechanism that governs methanol dehydrogenation on Ru surfaces in an aqueous environment. This mechanism, which can only be observed when explicit water molecules are bonded to the adsorbate, consists on a proton transfer from the hydroxyl group to nearby water molecules that dissociate afterward. Experimental and computational studies involving methanol dehydrogenation on Ru(0001) have only been done in vacuum.^{5,8,26,27} Our results are a step forward in describing the methanol decomposition pathway at the metal-water interface and can serve as a reference for further studies.

■ THEORETICAL METHODS

Simulated Systems. For each metal we consider two different situations: (1) no water molecules are added to the simulation box and (2) two water molecules are bonded to both methanol and the metal surface (see Figure 1a–f). For simplicity, we refer to these systems as CS (clean surface) and S2W (surface with two water molecules), respectively. The configuration of the two molecules for the later system is a chain so that the HOMO (basicity) of water is close enough to a water cluster value.²⁸ In both cases, the systems are also immersed in a continuum water medium simulated using the VASP-MGCM. As the water dissociation ratio on Ru(0001) is about 40 to 50%,²⁹ one water molecule is dissociated on the Ru S2W (Figure 1f). For Pt, we have also studied the decomposition path of methanol when it belongs to a solvated explicit ice-like water ring as that described in ref 29 (Figure 1g), both in vacuum and under solvation. We refer to this system as S5WR (surface with a five-water ring). The S5WR configuration is present in long-time simulations of liquid water (Born–Oppenheimer molecular dynamics, BOMD, at 300 K),²⁹ although other less structured 7-, 6-, and 5-membered rings are also present at the interface. At the same time, we have extracted a snapshot from the BOMD in ref 29 for the system containing the Pt surface (labeled as Pt4 in that reference) solvated by 72 water molecules. We replaced a flat water

molecule by methanol, preserving the hydrogen bonds that the replaced molecule had with its neighbors. Then, the adsorbate was relaxed along its vicinal water molecules (see Figure 1 h). This system is called S71W (surface with 71 water molecules). For the S5WR, the water configuration is reminiscent of that found around the methanol molecule in the S71W. Notice that unlike a water ring model coming from ice, the S5WR presents some molecules with the dipole moment slightly tilted with respect to the Pt surface. The S5WR retains then a certain degree of liquid-like behavior in the water configuration. Both the results for the S5WR and the S71W serve as a benchmark to assess the accuracy of the two strategies described above (CS and S2W).

Computational Details. DFT calculations were performed using the Vienna ab Initio Simulation Package (VASP),¹⁶ version 5.3.3, with the Perdew–Burke–Ernzerhof (PBE) GGA exchange-correlation functional.³⁰ Dispersion interactions were calculated through the semiempirical Grimme’s DFT-D2 method,³¹ with our reparameterized values for the metal atoms.³² Core electrons were described using the projector augmented wave (PAW) formalism,³³ while valence electrons were represented by plane waves with a cutoff energy of 450 eV. Solvent effects were treated through the VASP-MGCM. In this case, the value of the dielectric permittivity ϵ in the space is calculated using the Fattebert and Gygi functional form:³⁴

$$\epsilon(r) = \frac{\epsilon_0 - 1}{1 + (\rho_{el}(r)/\rho_0)^{2\beta}} \quad (1)$$

Here, ρ_{el} stands for the electronic charge density, ϵ_0 is the permittivity of the bulk phase of the solvent (78.5 for water), and ρ_0 and β are parameters controlling the shape of ϵ . The adopted values for these two parameters are $\beta = 1.7$ and $\rho_0 = 6 \times 10^{-4}$ a.u. The electronic convergence threshold was set to 10^{-5} and 10^{-6} eV for calculations involving metal surfaces and isolated molecules, respectively. In the case of gas-phase systems and the CS, the initial configurations were relaxed until forces acting on ions were lower than 30 meV/Å (15 meV/Å for solvated and unsolvated isolated molecules). In this case, a conjugate-gradient (CG) algorithm³⁵ was used to relax the ions into their instantaneous ground state. When explicit water molecules were adsorbed on the metal surfaces, the convergence criterion for the forces was slightly changed to 50 meV/Å and a quasi-Newton algorithm³⁶ was used to relax the ions for solvated systems. The choice of such algorithm was based on the fact that, when considering a CG algorithm for ion relaxation, we observed that some water molecules tended to rotate too much due to the interaction with the implicit aqueous environment. The CS and S2W metal surfaces were modeled by a four-layers $2\sqrt{3} \times 2\sqrt{3} - R30^\circ$ slab separated by at least 13 Å of vacuum along the z-axis, with dipole corrections included along this direction. For the S5WR and the S71W, we used a $3\sqrt{3} \times 3\sqrt{3} - R30^\circ$ reconstruction. The two topmost layers were relaxed, while the bottom ones were fixed to the bulk distances. The lattice parameters for Pd, Pt, and Ru were 3.939, 3.968, and 3.629 Å, respectively, and $[c/a]_{Ru} = 1.581$, in good agreement with the experimental values: 3.878, 3.924, and 3.615 Å, and $[c/a]_{Ru} = 1.584$.³⁷ The Brillouin zone was sampled by $3 \times 3 \times 1$ (CS and S2W systems) and $2 \times 2 \times 1$ (S5WR and S71W systems) Γ -centered k-points meshes constructed through the Monkhorst–Pack scheme.³⁸ A Gaussian smearing function with a width of 0.03 eV was used to broaden the energy levels around the Fermi level. Finally, we performed

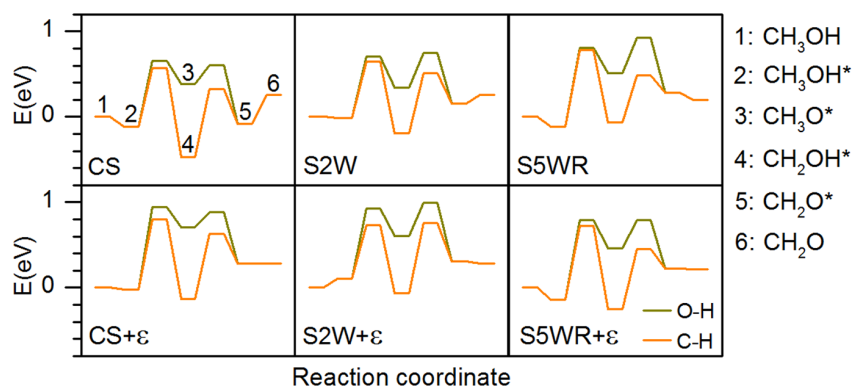


Figure 2. Reaction profiles for the dehydrogenation of methanol to CH_2O on Pt(111). ϵ stands for solvated systems. For clarity, all the intermediates are labeled.

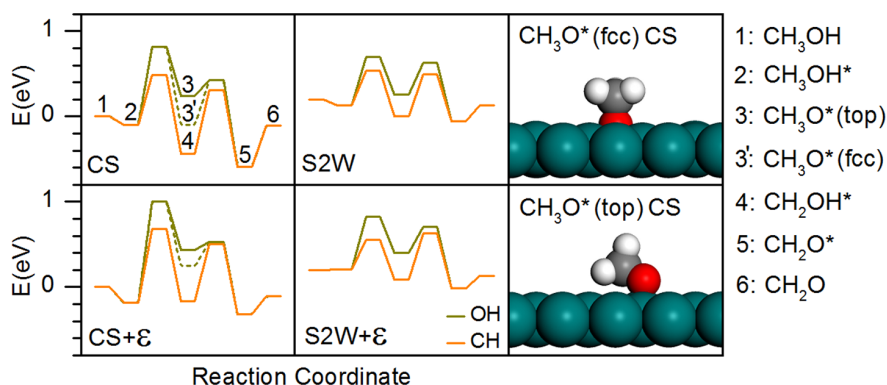


Figure 3. Reaction profiles for the dehydrogenation of methanol to CH_2O on Pd(111). The dashed line for the CS corresponds to the path starting with the O–H bond breaking but with the oxygen atom from the adsorbed methoxy tricoordinated to the Pd surface. ϵ stands for solvated systems. On the right panels we show the methoxy configurations on the CS (one of the H atoms is hidden due to the perspective); tricoordinated (top) and monocoordinated (bottom). For clarity, all the intermediates are labeled.

transition state (TS) searches through the improved dimer method (IDM).³⁹ A data set collection of computational results, including all the structures, is available in the ioChemBD repository.^{40,41}

RESULTS AND DISCUSSION

Pt(111). In Figure 2 we show the energy profile for methanol decomposition on Pt(111) for the different systems in vacuum and under solvation. The first step is the adsorption of methanol to the metal surface, described by the replacement energy, E_r , the energy cost of replacing a water molecule by methanol.

$$E_r^{0,\epsilon} = E_{m,s}^{0,\epsilon} + E_w^{0,\epsilon} - E_{w,s}^{0,\epsilon} - E_m^{0,\epsilon} \quad (2)$$

Here, $E_{m,s}$ is the energy of the system with adsorbed methanol, $E_{w,s}$ stands for the same system with a water molecule located at the methanol position, while E_m and E_w are the energies of the isolated methanol and water molecules, respectively. The superscript “0” denotes vacuum, while ϵ stands for the continuum-solvated. Adsorption energies for methanol on the CS in vacuum are provided in Section S1. Except for the S5WR, where the replacement is more exothermic in solution than in vacuum, the replacement energies increase when solvating the systems. Nevertheless, the values of E_r fall in the range $(-0.14, 0.11)$ eV, making the replacement of water by methanol almost thermoneutral. We have also calculated E_r for the S71W

in vacuum. In this case, $E_r = 0.09$ eV, a value that falls in the range of the error for all our measured replacement energies.

Solvent effects are found in the first dehydrogenation step. From now on, we call ΔE_a the difference in the height of the first activation barrier between the paths involving O–H and C–H bond breaking. That is, $\Delta E_a = E_{\text{TS}}^{\text{OH}} - E_{\text{TS}}^{\text{CH}}$, with $E_{\text{TS}}^{\text{OH}}$ and $E_{\text{TS}}^{\text{CH}}$ standing for the first transition state energies, respectively. In the three studied systems, there is an increase in ΔE_a under solvation with respect to what we observe in vacuum. This result agrees with both experimental and simulation data for methanol decomposition on Pt(111), where hydroxymethyl (H_2COH) becomes the most stable product in liquid.^{9–11} A commonly adopted explanation is that, under solvation, the methanol OH group has a larger number of water molecules around it as compared to the CH_3 group.⁹ This situation reduces the probability of the binding of the OH group to the Pt surface catalytic sites and favors the C–H bond breaking. To account for this fact, it is specially important to include explicit water molecules near the OH group in order to reproduce part of its first solvation shell. This strategy, adopted in the S2W, limits the methanol OH group mobility and its further binding to the Pt surface. Increasing the number of explicit molecules further does not improve the model, as ΔE_a is very small (0.06 eV under solvation and 0.03 eV in vacuum), and thus, both C–H and O–H bond breakings are possible in contrast with the experimental observation. This result is due to the strong rigidity imposed by the S5WR model.

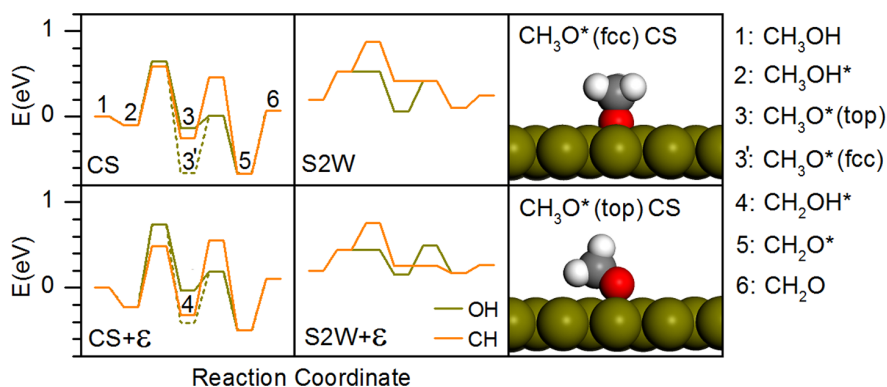


Figure 4. Reaction profiles for the dehydrogenation of methanol to CH_2O on $\text{Ru}(0001)$. The dashed line for the CS corresponds to the path starting with the O–H bond breaking but with the oxygen atom from the adsorbed methoxy tricoordinated to the Ru atoms. ϵ stands for solvated systems. On the right panels we show the methoxy configurations on the CS (one of the H atoms is hidden due to the perspective); tricoordinated (top) and monocoordinated (bottom). For clarity, all the intermediates are labeled.

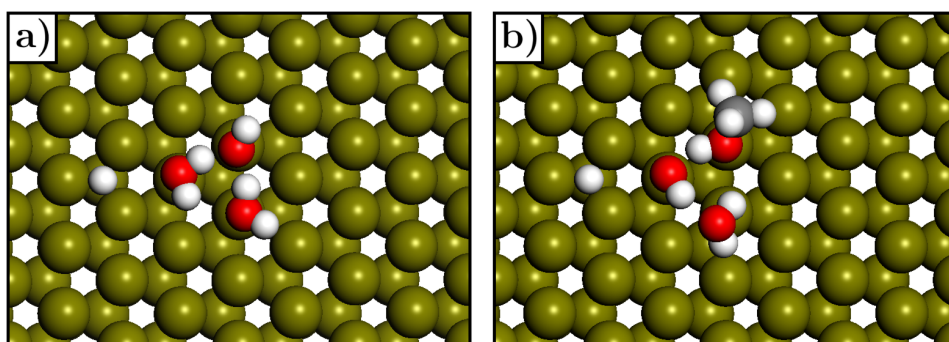


Figure 5. Adsorbate configuration for the S2W before methanol replaces a dissociated water molecule (a) and after methanol is adsorbed (b).

We have simulated a methanol trimer adsorbed on the CS to address cooperative effects. For the isolated molecules, the methanol cluster is more stable than the separated methanol molecules (both in vacuum and solvated by water). When the trimer is adsorbed on Pt, the methanol trimer is only more stable in vacuum but solvation renders separated methanol molecules more favorable (see Section S2). Therefore, O–H bond breaking cannot be favored through cooperative interactions on the surface if water is present.

The second dehydrogenation step under solvation is rather similar for the S2W and the S5WR systems. In particular, for the CH_3O dehydrogenation, the height of the barrier equals 0.17 and 0.39 eV for the CS and S2W, respectively, being this quantity for the S5WR equal to 0.33 eV. With regard to the CH_2OH dehydrogenation, both the CS and S2W yield similar results as compared to the S5WR.

Pd(111). The analysis of the energy profiles on $\text{Pd}(111)$ yields similar results to those for the Pt surface (see Figure 3). Regarding the replacement energies, E_r^c equals -0.19 and 0.01 eV for the CS and S2W, respectively, meaning that methanol adsorption is not much more preferred than desorption, even in an aqueous environment. The value of ΔE_a for the CS is the same for both solvated and unsolvated systems ($\Delta E_a = 0.33$ eV). However, ΔE_a increases by 0.16 eV for the S2W when solvating the system (from 0.24 eV in vacuum to 0.40 eV under solvation). The first activation barrier for the C–H bond breaking decreases from 0.61 eV (vacuum) to 0.53 eV (solvation). These results indicate that, like in Pt, the C–H

bond breaking becomes the preferential mechanism in aqueous environment.

With respect to the configuration of the adsorbed CH_3O there is a difference between the Pd CS and S2W (see Figure 3). For the CS, the configuration with the oxygen atom coordinated to a fcc site (tricoordinated structure) is 0.34 eV more stable in vacuum than that with the oxygen atom coordinated to a top site (monocoordinated structure, see dashed line in Figure 3). When solvating the tricoordinated geometry, the energy decreases by 0.19 eV with respect to the flat situation due to the three available hydrogen atoms that the implicit solvent has to interact with. The scenario is quite different for the S2W as the water molecules maintain the adsorbate configuration flat and close to the surface. This adsorption reordering is the most serious reason to include explicit water molecules in any calculation under solvation.

Ru(0001). Water dissociates on Ru surfaces (dissociation ratio of about 40 to 50%), which might have an effect on methanol decomposition. For instance, explicit water molecules have been taken into account to study the conversion of levulinic acid on this surface.^{42,43} In Figure 4 we show the energy profile for methanol dehydrogenation on the Ru surfaces. For the CS $E_r^c = -0.22$ eV (in vacuum, $E_r^0 = -0.09$ eV). Solvating the system increases ΔE_a in 0.20 eV with respect to the vacuum situation, and therefore, the C–H bond breaking becomes the most favored methanol first decomposition mechanism. The exothermic character of the methanol O–H bond breaking depends, however, on the orientation of the C–O bond with respect to the surface plane. This issue, which

is inherent to the CS, becomes more clear for the solvated system where the reaction is exothermic if the C–O bond is perpendicular to the surface plane and endothermic when the C–O bond is parallel to it. The net effect of taking the tricoordinated CH₃O structure is an increase in the height of the activation barrier for its dehydrogenation of 0.53 and 0.38 eV for the unsolvated and solvated systems, respectively.

The situation changes drastically when we add two water molecules (one dissociated) to the simulation box. On the reference S2W (that with two water molecules and an OH, see Figure 5a) the oxygen atom from the dissociated water is hydrogen-bonded at the same time to two hydrogen atoms. When methanol replaces the dissociated water, one of the remaining two water molecules becomes an OH group (see Figure 5b). Then, the global hydrogen bond network becomes slightly more distorted than for the previous situation making the methanol adsorption more endothermic than on the Pd and Pt surfaces ($E_r^0 = 0.49$ eV and $E_r^e = 0.37$ eV). With regard to the methanol first dehydrogenation step, the O–H bond breaking is barrierless as the proton is transferred to the nearest water molecule (which is a dissociated water) and then the newly formed water molecule dissociates. This situation is not observed for the path involving the C–H bond breaking, where the activation barrier equals 0.52 and 0.46 eV for the unsolvated and solvated systems, respectively. These results give us some clues about the mechanism that governs methanol decomposition on Ru. This fact reinforces not only the need for the addition of two water molecules to the simulation box but also the importance of adopting a configuration such as that in Figure 5b. With regard to the CH₂OH dehydrogenation, it is also an inactivated process due to the proton transfer from the OH group to a water molecule. In this case, solvating the system involves that the surface with the adsorbed CH₂OH has a similar energy to that with the adsorbed CH₂O (0.13 eV of difference). For the CH₃O dehydrogenation, however, adding the solvent does not involve a large change in the barrier (–0.04 eV).

To compile the results, a comparison between the three surfaces can be drawn. We have found that (i) for Pd and Pt the methanol C–H bond breaks first, whereas the O–H bond breaking is the first step on Ru, (ii) the number of explicit water molecules needed is the same for all surfaces, (iii) although the S5WR ring structures are slightly more flexible than the ice-derived ones, they might still be too rigid to represent the aqueous environments found in ref 29 where 5-, 6- and 7-membered rings also appear, and (iv) the models used to study water-assisted processes on Ru need to account for the dissociation of some water molecules.

CONCLUSIONS

We have employed first-principles calculations to study the methanol dehydrogenation path to formaldehyde on Pd(111), Pt(111), and Ru(0001) under aqueous environment. In particular, we have adopted a combined explicit/implicit solvation approach. The results for the methanol dehydrogenation profiles on solvated Pd and Pt surfaces agree with experiments where the methanol C–H bond breaking is the preferred first dehydrogenation step. This situation is attributed to the fact that the methanol CH groups in solution are more exposed to the metal surface atoms than the OH group, which favors the C–H bond breaking. The calculated reaction profiles for the surface containing two explicit water molecules (S2W) qualitatively agree with those calculated for a benchmark

system, the S5WR (surface with a five-water ring) where the methanol environment is close to that encountered on systems with several explicit water layers. The addition of two explicit water molecules also prevents the intermediates to adopt undesired configurations (specially for the case of the CH₃O in Pd and Ru in the CS) that result in overestimated values for the activation energies. Water dissociation on Ru(0001) makes the methanol decomposition very different from the case of Pd and Pt surfaces. The dehydrogenation of methanol on the Ru S2W occurs via a proton transfer from the methanol OH group to a nearby water molecule that dissociates afterward. This makes the methanol O–H bond breaking to become barrierless. No theoretical results exist for the dehydrogenation of methanol on solvated Ru(0001), and therefore, the aforementioned mechanism can serve as a reference for further studies. Notice that the water dissociation at the Ru interface is crucial to address the catalytic properties of this particular surface that is extensively used, for instance, in the conversion of levulinic acid to gamma-valerolactone.⁴³ Our results show the need to include both implicit and explicit water molecules in the computational box and thus pave the way toward faster and more reliable simulations in catalytic and electrochemical reactions on surfaces.

ASSOCIATED CONTENT

Supporting Information

In Section S1, we provide the data associated with the energy profiles for the methanol dehydrogenation, that is methanol adsorption and replacement energies, and desorption energies of formaldehyde as well as activation and reaction energies; in Section S2, we give the energies for the clustered methanol species on metal surfaces (PDF)

AUTHOR INFORMATION

Corresponding Authors

*E-mail: mgarcia@iciq.es.

*E-mail: nlopez@iciq.es. Phone: +34 977 920237. Fax: +34 977 920231.

ORCID

Miquel Garcia-Ratés: 0000-0002-6315-0845

Rodrigo García-Muelas: 0000-0002-2219-5027

Núria López: 0000-0001-9150-5941

Notes

The authors declare no competing financial interest.

ACKNOWLEDGMENTS

The authors acknowledge the European Research Council (ERC-2010-StG-258406) and MINECO (projects CTQ2012-33826 and CTQ2015-68770-R) for financial support and BSC-RES for providing generous computer resources.

REFERENCES

- (1) Huber, G. W.; Iborra, S.; Corma, A. Synthesis of Transportation Fuels from Biomass: Chemistry, Catalysts, and Engineering. *Chem. Rev.* **2006**, *106*, 4044–4098.
- (2) Larminie, J.; Dicks, A. *Fuel Cell Systems Explained*; John Wiley & Sons: Chichester, U.K., 2003.
- (3) Martin, R. M. *Electronic Structure: Basic Theory and Practical Methods*; Cambridge University Press: Cambridge, U.K., 2004.

- (4) Akhter, S.; White, J. M. A Static SIMS/TPD Study of the Kinetics of Methoxy Formation and Decomposition on O/Pt(111). *Surf. Sci.* **1986**, *167*, 101–126.
- (5) Barros, R.; Garcia, A.; Ilharco, L. The Decomposition Pathways of Methanol on Clean Ru(0001), Studied by Reflection-Absorption Infrared Spectroscopy (RAIRS). *J. Phys. Chem. B* **2001**, *105*, 11186–11193.
- (6) Desai, S. K.; Neurock, M.; Kourtakis, K. A Periodic Density Functional Theory Study of the Dehydrogenation of Methanol over Pt(111). *J. Phys. Chem. B* **2002**, *106*, 2559–2568.
- (7) Greeley, J.; Mavrikakis, M. Competitive Paths for Methanol Decomposition on Pt(111). *J. Am. Chem. Soc.* **2004**, *126*, 3910–3919.
- (8) García-Muelas, R.; Li, Q.; López, N. Density Functional Theory Comparison of Methanol Decomposition and Reverse Reactions on Metal Surfaces. *ACS Catal.* **2015**, *5*, 1027–1036.
- (9) Franaszczuk, K.; Herrero, E.; Zelenay, P.; Wieckowski, A.; Wang, J.; Masel, R. I. A Comparison of Electrochemical and Gas-Phase Decomposition of Methanol on Platinum Surfaces. *J. Phys. Chem.* **1992**, *96*, 8509–8516.
- (10) Sakong, S.; Groß, A. The Importance of Electrochemical Environment in the Electro-Oxidation of Methanol on Pt(111). *ACS Catal.* **2016**, *6*, 5575–5586.
- (11) Herron, J. A.; Morikawa, Y.; Mavrikakis, M. Ab Initio Molecular Dynamics of Solvation Effects on Reactivity at Electrified Interfaces. *Proc. Natl. Acad. Sci. U. S. A.* **2016**, *113*, E4937–E4945.
- (12) Neurock, M.; Wasileski, S. A.; Mei, D. From First Principles to Catalytic Performance: Tracking Molecular Transformations. *Chem. Eng. Sci.* **2004**, *59*, 4703–4714.
- (13) Hartnig, C.; Spohr, E. The Role of Water in the Initial Steps of Methanol Oxidation on Pt(111). *Chem. Phys.* **2005**, *319*, 185–191.
- (14) Frenkel, D.; Smit, B. *Understanding Molecular Simulation, from Algorithms to Applications*, 2nd ed.; Academic: San Diego, CA, 1996.
- (15) Tomasi, J.; Mennucci, B.; Cammi, R. Quantum Mechanical Continuum Solvation Models. *Chem. Rev.* **2005**, *105*, 2999–3093.
- (16) Kresse, G.; Furthmüller, J. Efficiency of Ab-Initio Total Energy Calculations for Metals and Semiconductors Using a Plane-Wave Basis Set. *Comput. Mater. Sci.* **1996**, *6*, 15–50.
- (17) Garcia-Ratés, M.; López, N. Multigrid-Based Methodology for Implicit Solvation Models in Periodic DFT. *J. Chem. Theory Comput.* **2016**, *12*, 1331–1341.
- (18) Diez, J.; Gimeno, J.; Lledós, A.; Suárez, F. J.; Vicent, C. Imidazole Based Ruthenium(IV) Complexes as Highly Efficient Bifunctional Catalysts for the Redox Isomerization of Allylic Alcohols in Aqueous Medium: Water as Cooperating Ligand. *ACS Catal.* **2012**, *2*, 2087–2099.
- (19) Ortuño, M. A.; Lledós, A.; Maseras, F.; Ujaque, G. The Transmetalation Process in Suzuki-Miyaura Reactions: Calculations Indicate Lower Barrier via Boronate Intermediate. *ChemCatChem* **2014**, *6*, 3132–3138.
- (20) Fang, Y.-H.; Wei, G.-F.; Liu, Z.-P. Constant-Charge Reaction Theory for Potential-Dependent Reaction Kinetics at the Solid-Liquid Interface. *J. Phys. Chem. C* **2014**, *118*, 3629–3635.
- (21) Zaffran, J.; Michel, C.; Delbecq, F.; Sautet, P. Towards More Accurate Prediction of Activation Energies for Polyalcohol Dehydrogenation on Transition Metal Catalysts in Water. *Catal. Sci. Technol.* **2016**, *6*, 6615–6624.
- (22) Wei, G.-F.; Fang, Y.-H.; Liu, Z.-P. First Principles Tafel Kinetics for Resolving Key Parameters in Optimizing Oxygen Electrocatalytic Reduction Catalyst. *J. Phys. Chem. C* **2012**, *116*, 12696–12705.
- (23) He, Z.-D.; Hanselman, S.; Chen, Y.-X.; Koper, M. T. M.; Calle-Vallejo, F. Importance of Solvation for the Accurate Prediction of Oxygen Reduction Activities of Pt-Based Electrocatalysts. *J. Phys. Chem. Lett.* **2017**, *8*, 2243–2246.
- (24) Sakong, S.; Naderian, M.; Mathew, K.; Hennig, R. G.; Groß, A. Density Functional Theory Study of the Electrochemical Interface between a Pt Electrode and an Aqueous Electrolyte Using an Implicit Solvent Method. *J. Chem. Phys.* **2015**, *142*, 234107.
- (25) Bodenschatz, C. J.; Sarupria, S.; Getman, R. B. Molecular-Level Details about Liquid H₂O Interactions with CO and Sugar Alcohol Adsorbates on Pt(111) Calculated Using Density Functional Theory and Molecular Dynamics. *J. Phys. Chem. C* **2015**, *119*, 13642–16351.
- (26) Gazdzicki, P.; Jakob, P. Reactions of Methanol on Ru(0001). *J. Phys. Chem. C* **2010**, *114*, 2655–2663.
- (27) Lu, X.; Wang, W.; Deng, Z.; Zhu, H.; Wei, S.; Ng, S. P.; Guo, W.; Wu, C. M. L. Methanol Oxidation on Ru(0001) for Direct Methanol Fuel Cells: Analysis of the Competitive Reaction Mechanism. *RSC Adv.* **2016**, *6*, 1729–1737.
- (28) Bellarosa, L.; Castillo, J. M.; Vlugt, T.; Calero, S.; López, N. On the Mechanism Behind the Instability of Isorecticular Metal-Organic Frameworks (IRMOFs) in Humid Environments. *Chem. - Eur. J.* **2012**, *18*, 12260–12266.
- (29) Bellarosa, L.; García-Muelas, R.; Revilla-López; López, N. Diversity at the Water-Metal Interface: Metal, Water Thickness, and Confinement Effects. *ACS Cent. Sci.* **2016**, *2*, 109–116.
- (30) Perdew, J. P.; Burke, K.; Ernzerhof, M. Generalized Gradient Approximation Made Simple. *Phys. Rev. Lett.* **1996**, *77*, 3865–3868.
- (31) Grimme, S. Semiempirical GGA-Type Density Functional Constructed with a Long-Range Dispersion Correction. *J. Comput. Chem.* **2006**, *27*, 1787–1799.
- (32) Almora-Barrios, N.; Carchini, G.; Błóński, P.; López, N. Costless Derivation of Dispersion Coefficients for Metal Surfaces. *J. Chem. Theory Comput.* **2014**, *10*, 5002–5009.
- (33) Blöchl, P. E. Projector Augmented-Wave Method. *Phys. Rev. B: Condens. Matter Mater. Phys.* **1994**, *50*, 17953–17979.
- (34) Fattebert, J.-L.; Gygi, F. Density Functional Theory for Efficient Ab Initio Molecular Dynamics Simulations in Solution. *J. Comput. Chem.* **2002**, *23*, 662–666.
- (35) Press, W. H.; Teukolsky, S. A.; Vetterling, W. T.; Flannery, B. P. *Numerical Recipes in Fortran 90. The Art of Parallel Scientific Computing*, 2nd ed.; Cambridge University Press: New York, 1999.
- (36) Pulay, P. Convergence Acceleration of Iterative Sequences. The Case of SCF Iteration. *Chem. Phys. Lett.* **1980**, *73*, 393–398.
- (37) Lide, D. R. *CRC Handbook of Chemistry and Physics*, 84th ed.; CRC Press LLC: Boca Raton, FL, 2003.
- (38) Monkhorst, H. J.; Pack, J. D. Special Points for Brillouin-Zone Integrations. *Phys. Rev. B* **1976**, *13*, 5188–5192.
- (39) Heyden, A.; Bell, A. T.; Keil, F. J. Efficient Methods for Finding Transition States in Chemical Reactions: Comparison of Improved Dimer Method and Partitioned Rational Function Optimization Method. *J. Chem. Phys.* **2005**, *123*, 224101.
- (40) Álvarez-Moreno, M.; de Graaf, C.; López, N.; Maseras, F.; Poblet, J. M.; Bo, C. Managing the Computational Chemistry Big Data Problem: The ioChem-BD Platform. *J. Chem. Inf. Model.* **2015**, *55*, 95–103.
- (41) Data-set collection of computational results, including all the structures. <https://doi.org/10.19061/iochem-bd-1-39> (accessed June 8, 2017).
- (42) Steinmann, S. N.; Sautet, P.; Michel, C. Solvation Free Energies for Periodic Surfaces: Comparison of Implicit and Explicit Solvation Models. *Phys. Chem. Chem. Phys.* **2016**, *18*, 31850–31861.
- (43) Albani, D.; Li, Q.; Vilé, G.; Mitchell, S.; Almora-Barrios, N.; Witte, P. T.; López, N.; Pérez-Ramírez, J. Interfacial acidity in Ligand-Modified Ruthenium Nanoparticles Boosts the Performance for the Continuous Hydrogenation of Levulinic Acid to Gamma-Valerolactone. *Green Chem.* **2017**, *19*, 2361–2370.